Available online at www.sciencedirect.com
ScienceDirect
Earth and Planetary Science Letters 249 (2006) 350–367
EPSL
www.elsevier.com/locate/epsl

Late Cenozoic uplift of the Eastern Cordillera, Bolivian Andes

Richard Barke [1], Simon Lamb *

Department of Earth Sciences, Parks Road, Oxford, OX1 3PR, England, UK

Received 23 March 2006; received in revised form 7 July 2006; accepted 10 July 2006
Available online 22 August 2006
Editor: Scott King

Abstract

This paper analyses Late Cenozoic uplift in the Bolivian Andes, using the morphology of well preserved regional paleosurfaces in the Eastern Cordillera that define three axially draining braided river catchments that formed between ~12 and ~9 Ma. Rock uplift since the formation of the paleodrainage systems, which has been quantified using four different methods, is 1705±695 m, with a mean erosion of 230±90 m as a consequence of entrenchment of the drainage systems. The lack of faulting or tilting in the regions immediately farther west strongly suggest that rock uplift of the paleodrainage systems also extends to the western margin of the Eastern Cordillera. Balanced structural cross-sections require crustal deformation at depth beneath the Eastern Cordillera, in order to accommodate underthrusting of the Brazilian Shield beneath the thin-skinned fold and thrust belt on the eastern margin of the Bolivian Andes. In this case, the observed uplift of the Eastern Cordillera is easily explained by sliding up a ramp in the major decollement, dipping in the range 4°–16°W, as a consequence of the observed 60–110 km of shortening farther east, in the Subandean zone. Contemporaneous uplift of the western margin of the Eastern Cordillera is easily explained in terms of crustal thickening as a result of ductile squeezing in the lower crust accommodating at depth the Subandean shortening. It remains unclear how this uplift relates to that of the regions farther west, in the Altiplano and volcanic arc, except that uplift in the Eastern Cordillera coincides with a phase of intense shortening in the northern Altiplano, commencing at ~9.5 Ma and continuing to ~2.7 Ma and possibly younger.

Keywords: Andes; Late Cenozoic; tectonics; uplift; crust

1. Introduction

An important problem in geology is the causes of large elevation contrasts in the continents, and particularly the rise of mountain belts. The principle of isostasy requires the surface elevation of a continent to be related to the underlying density structure in the lithosphere. The main density contrast is between the crust and mantle, and so an increase in crustal thickness, either through crustal shortening or magmatic addition, will have a first order effect on surface elevation. Processes of lithospheric thinning, such as the replacement of lithospheric mantle with lower density asthenosphere, or delamination of a high density lower crust, could also lead to a significant increase in surface elevation [1,2].

One way to assess the relative roles of these various mechanisms is to compare the history of crustal shortening with crustal thickness and uplift [3,4]. Here, we do this by exploiting the constraints on crustal structure,

* Corresponding author. Tel.: +44 1865 272035; fax: +44 1865 272072.
E-mail address: simon.lamb@earth.ox.ac.uk (S. Lamb).
[1] Now at ExxonMobil, Union Row, Aberdeen, AB10 1SA.

0012-821X/$ - see front matter © 2006 Elsevier B.V. All rights reserved.
doi:10.1016/j.epsl.2006.07.012

uplift and shortening since the Late Miocene in the Eastern Cordillera of the Bolivian Andes (Fig. 1) [5–9]. First, we use the morphology of well preserved Late Miocene paleodrainage systems in the Eastern Cordillera (Fig. 2) to provide the best possible constraints on uplift since these systems were active; then we investigate simple models of crustal deformation and uplift in the Eastern Cordillera, using new estimates of crustal shortening [9]. We show that uplift of the order of kilometres since the Late Miocene should be anticipated simply as a consequence of crustal thickening, without the need for large scale changes in the underlying mantle structure.

1.1. Surface uplift, rock uplift and exhumation

It is important to distinguish between surface uplift U_s and rock uplift U_r. Surface uplift is the average uplift of portions (area at least 10^3–10^4 km^2) of the Earth's surface with respect to the geoid, whereas rock uplift refers to the uplift of a particle of rock. Therefore, $U_s = U_r - E$, where the exhumation E is the average thickness of material

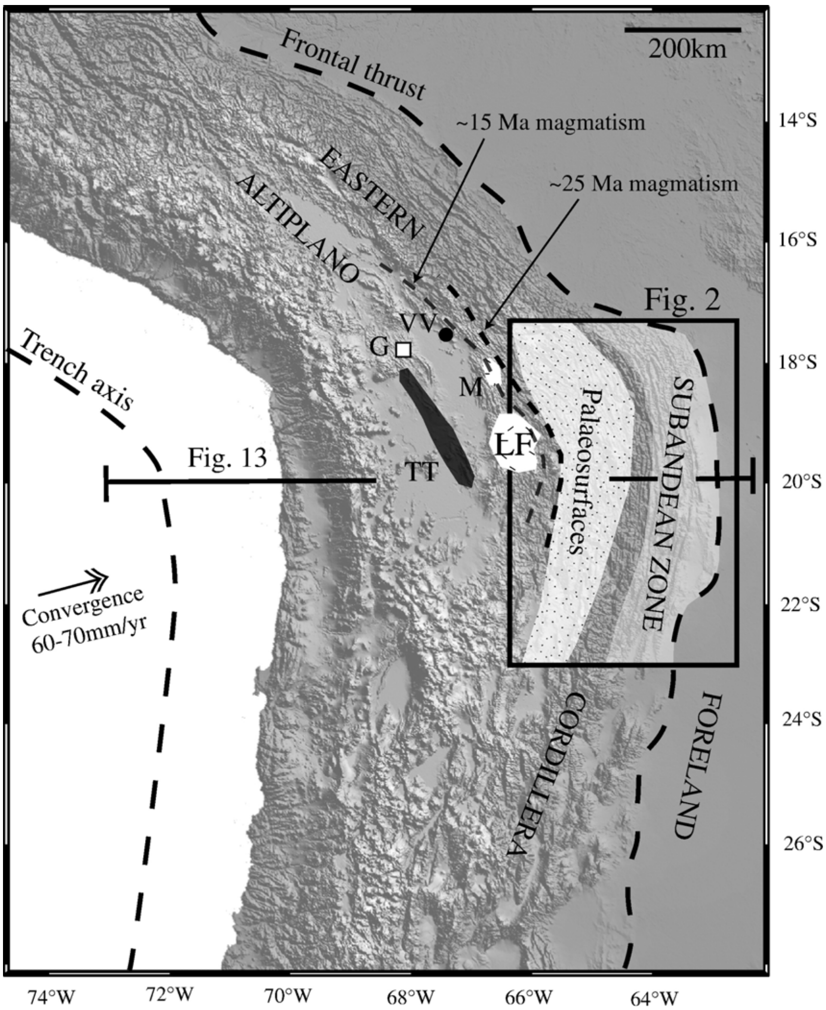

Fig. 1. Map showing the tectonic setting and topography of the Central Andes. Box shows the location of the study area (see Fig. 2). The Altiplano forms a high plateau. Farther east, in the Eastern Cordillera, well-preserved and undeformed paleosurfaces are the remnants of a once extensive Late Miocene paleodrainage system, whereas the Subandean zone is a thin-skinned fold and thrust belt that has undergone intense shortening since the Late Miocene. Small dashed lines show easternmost limit of ~25 Ma and ~15 Ma magmatism. The undeformed 12–1.5 Ma Los Frailes volcanic complex (LF) and 24–10 Ma older stocks and intrusions and 9–5 Ma Morococala ignimbrites (M) outcrop to the west of the paleosurface remnants. The location of voluminous Altiplano mafic magmatism is shown in black (TT = 25–22 Ma Tambo Tambillo basic lavas and intrusions; VV = 13–11 Ma Vila Vila shoshonitic lava field). White square shows location of Garcione et al.'s [2] paleoaltimetry study. See Fig. 13 for regional cross-section.

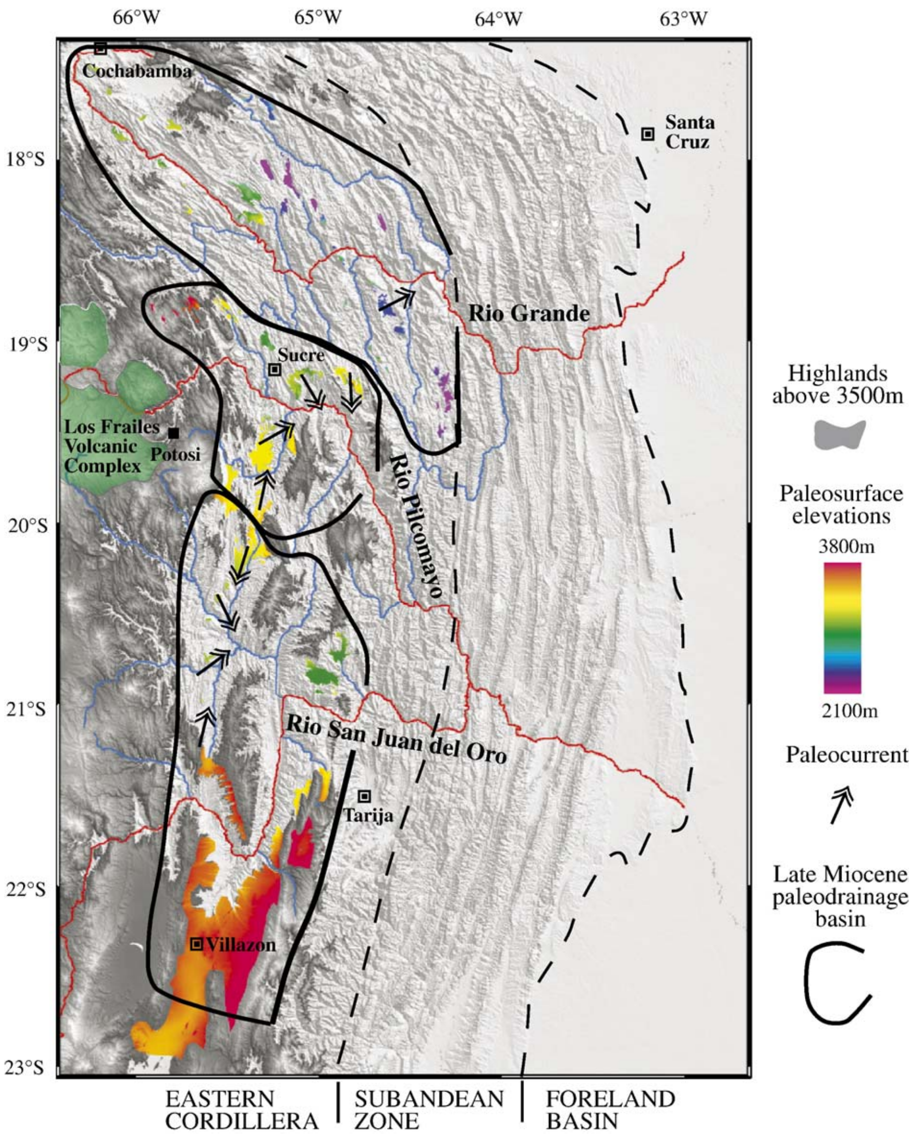

Fig. 2. Summary map showing the remnants of Late Miocene paleodrainage systems in the Eastern Cordillera. These are defined by low relief paleosurfaces dated to ~12–~9 Ma [9]. The surface remnants are colour coded according to elevation, while highland regions, above the paleosurface elevations, are shown in darker grey. Three paleodrainage systems can be defined (outlined with bold lines), based on paleoflow data for aggradational gravels that cap the surfaces. The paleodrainage systems essentially coincide with the catchments for the existing main rivers in the Eastern Cordillera (Rio Grande, Pilcomayo and San Juan del Oro rivers, shown in red), and they all flowed into the Late Miocene foreland basin on the western margin of the Subandean zone. The 24–1.5 Ma Los Frailes volcanic complex and older intrusions and stocks (shown in green) outcrop to the west of the paleodrainage systems.

removed from the Earth's surface through either erosion or tectonic processes.

Published estimates of U_r in the Bolivian Andes since the Mid-Miocene are mainly based on paleobotanical studies in the Altiplano and Eastern Cordillera (Table 1, [10–13]). The method relies on a quantitative association between floras, climate and elevation, and has large errors which arise principally from uncertainties in the link between climate and elevation. Kennan et al. [14] compared the elevations of modern rivers in the Eastern Cordillera with the elevations of paleosurfaces created by Late Miocene paleodrainage systems (Table 1). Recently, Garzione et al. [2] have used the oxygen isotope ratios in carbonates in a ~11 Ma to 5 Ma red-bed sequence, in the northern Bolivian Altiplano, to estimate the elevation of carbonate precipitation. All these methods have errors in excess of a kilometre, in addition to unquantifiable systematic errors. However, taken together, the estimates

Table 1
Mid-Miocene to recent rock uplift estimates for the Central Andes

Method[a]	Locality	Region[b]	Age (Ma)	Paleoelevation (m)	Modern elevation (m)	Uplift (m)	Reference[c]
Palaeobotany: NLR	Corocoro	A	10–15	2000±2000	4000	2000±2000	[1]
	Potosi	EC	13.8–20.8	2800±2000	4300	1500±2000	[2]
Palaeobotany: FP	Potosi	A	13.8–20.8	0–1320±1200	4300	3040±1260	[3]
	Jakokkota	A	10–11	590–1610±1200	3940	2535±1405	[3]
	Pislepampa	EC	6–7	1200–1400±1000	3600	2300±1100	[4]
Drainage evolution	EC	EC	12–9	1000–1500±1000	~3250	1950±1250	[5]
	EC	EC	12–9	350–1880	~3250	1705±675	This study
Carbonate geochemistry	Callapa	A	10.3–6.7	0–1500	3900	2400–3900	[6]

Notes: a NLR = nearest-living-relative method, FP = foliar physiognomic method.
b A = Altiplano, EC = Eastern Cordillera.
c References: [1] = Singewald and Berry [10]; [2] = Berry [11]; [3] = Gregory-Wodzicki [12]; [4] = Graham et al. [13]; [5] = Kennan et al. [14]; [6] = Garzione et al. [2]. Each individual estimate has large error bounds, but put together there is a suggestion of uplift of the order of 1.5 to 2.5 km.

would suggest a rock uplift much greater than 1 km since ~10 Ma.

1.2. Paleosurfaces in the Eastern Cordillera of the Bolivian Andes

Barke [9] used a combination of extensive field observations, Landsat-7 satellite images, and a hydrologically correct 90 m digital elevation model, to constrain the morphology of well preserved erosional or depositional low relief paleosurfaces in the Eastern Cordillera [7,14,15]. This work has shown that the remnants comprise low relief erosional surfaces together with depositional surfaces underlain by conglomeratic sequences ≤120 m thick. Their morphology and sedimentology define three axially draining braided river catchments (Fig. 2, San Juan de Oro, Pilcomayo, and Rio Grande basins), extending for ~500 km along the length of the Eastern Cordillera, and preserved virtually intact except for deep dissection (see Section 1.2.1).

Dated tuff horizons within associated gravels, or in incised valleys [7,9,14,15] show that paleodrainage systems were mainly active between ~12 and ~9 Ma. The drainage in its early stages was mainly erosive, producing widespread planation surfaces, mainly cut into Paleozoic bedrock. But by ~9 Ma, significant aggradation resulted in the accumulation of conglomerate sequences, reaching 120 m thick in places. Significant entrenchment of the rivers had occurred by 6.5 Ma, so that today the paleosurfaces are deeply dissected, with remnants found at an average elevation of ~3250 m and generally more than 1000 m higher than the present rivers along their eastern margins.

1.2.1. Deformation of paleosurfaces

The paleosurfaces appear to be essentially undeformed and untilted, preserving, more-or-less intact, the surface slopes and directions of the paleodrainage systems that created them [9]. Paleocurrent data show that aggradational conglomerates, overlying erosion surfaces, were deposited by rivers conforming both to the modern drainage pattern, and also the gradients of the paleosurfaces themselves, with the majority of the flow being axial, parallel to the structural grain of the Eastern Cordillera, and with no paleoflow across modern drainage divides (Figs. 2 and 3), and paleosurface gradients similar to those in modern, low gradient rivers in the Bolivian Andes (see Section 2.1.2). The thickest aggradational conglomerate sequences are found in the lowest parts of the catchment, and the present

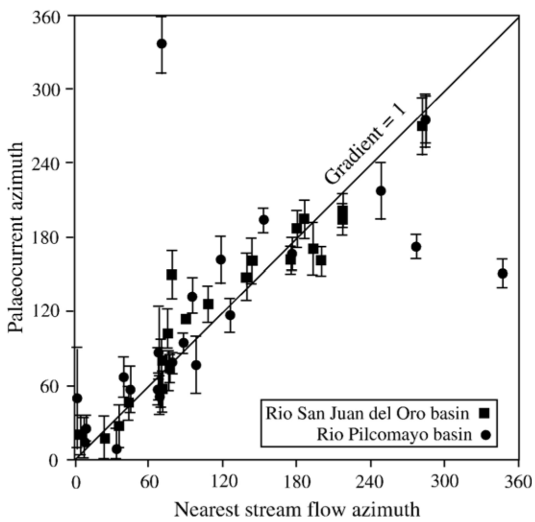

Fig. 3. A plot of Late Miocene paleodrainage flow azimuths (with 95% confidence limits), from clast imbrication in ~9 Ma conglomerates, against the flow azimuth of the nearest modern river. Paleocurrent data shows a remarkable 1:1 correlation with modern drainage, indicating that the modern stream network is a good approximation of the paleodrainage, presumably because the paleorivers simply entrenched into their beds during uplift. Also, the paleosurface remnants cannot have been substantially warped or tilted.

entrenched rivers do not seem to be biased significantly to either side of the region of the paleosurfaces.

Deformation of the paleosurfaces is only local and minor, such as rare small (<10 m) vertical offsets, strike-slip faulting with no vertical offsets, and mainly confined to the northernmost paleosurface remnants in the core of the Bolivian orocline [9,16–18]. In addition, the aspects of paleosurfaces, defined as the direction of downhill slope, show a remarkably uniform distribution, strongly suggesting that the surfaces have not been tilted in any preferred direction, and especially about a north–south axis, parallel to the dominant drainage direction [9]. Farther west, the symmetrical morphology of the contemporaneous Los Frailes volcanic complex also suggests negligible tilting in the region adjacent to the paleosurface remnants in the last ~10 Ma [9].

1.2.2. Paleodrainage base level

Over the last ~10 Ma, deformation in the Subandean zone, on the eastern margin of the Bolivian Andes, has steadily encroached into the foreland basin [5–7,9,19–22], as the front of the Andes has advanced eastward. For this reason, the position of the foreland, at the time when the paleodrainage system was active, must have been much closer to the back of the Subandean fold and thrust belt and ~50 km east of the most eastern extent of the paleosurfaces today (Figs. 1 and 2).

There is clear evidence that the paleodrainage systems flowed into this foreland basin: (1) the lack of any topographic barrier between the paleosurface remnants and the Subandean zone [9]; (2) only thin conglomerate deposits (generally <100 m) in paleodrainage catchments, and much less than expected for planation of the Eastern Cordillera, where peaks rise >1000 m above paleosurfaces [9]; (3) no lacustrine or evaporitic deposits, typical of internal drainage basins [9,14]; (4) rapid increase in deposition in the foreland basin at ~9 Ma when the paleodrainage was itself aggrading [16], and shortening in the Subandean zone was starting or markedly increasing. Thus, the base level for the paleodrainage basins is the level of the foreland basin. Today, this is at an average elevation of ~300 m (Fig. 4, [9]), but may have been nearer to sea-level at ~10 Ma, when marine and mud-flat facies were deposited in the foreland basin [19–22]. In this study, we asssume that the base level has remained unchanged.

2. Estimating rock uplift of the paleodrainage systems in the Eastern Cordillera

We use four approaches to constrain the original elevation of the paleodrainage systems. Three of these give an upper bound on the subsequent amount of rock uplift, because they assume smooth downstream paleoriver profiles from the Eastern Cordillera into the foreland basin. The presence of knickpoints in the paleodrainage systems will affect these estimates, and a lower bound on the amount of rock uplift is given by considering the maximum possible amplitude of knickpoints.

The estimates are summarised in Table 2, and discussed in detail in the following sections. Taken together, they suggest 1705±695 m of rock uplift since the paleodrainage systems formed at ~12–9 Ma.

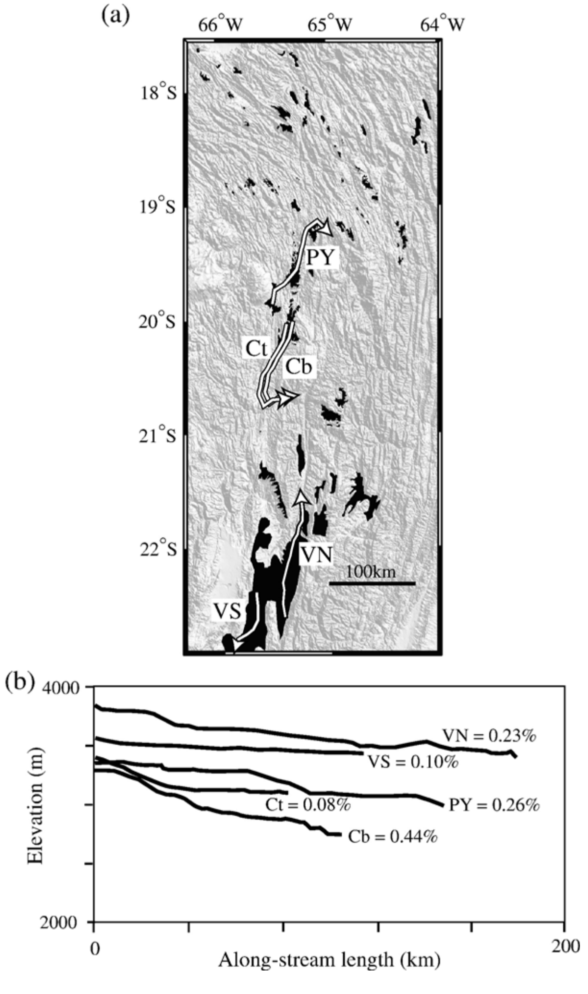

Fig. 4. Paleoriver profiles across paleosurfaces in the Eastern Cordillera. (a) The locations of 5 profiles (overlain on SRTM: 90 m digital elevation model, paleosurface remnants in black). Arrows indicate the downstream direction. (b) Along-stream profiles of the 5 profiles in (a): PY = Puna–Yamparez profile, Cb = Cotagaita-base profile, Ct = Cotagaita-top profile, VN = Villazon-N profile, VS = Villazon-S profile. Along-stream gradients range from 0.2% to 0.5% for the erosional surface remnants. Note that the paleodrainage is predominantly north–south, parallel to the general structural trend of the Eastern Cordillera.

2.1. Along-stream river gradients

This approach assumes that the original elevations of the paleodrainage systems (above their base level) are the same as the elevations (above base level, in the foreland) of those reaches of the modern river system that have similar gradients to the paleodrainage systems.

The average along-stream gradient of the paleorivers is equal to the change in height divided by the along-stream distance. The change in height is measured directly from the digital elevation model; however determining the along-stream lengths to assign to the heights is not so straightforward. Given the very close similarity between the modern and paleodrainage patterns and catchment areas, because the rivers entrenched into their own beds, we use the along-stream lengths of the nearest modern rivers as a proxy for the along-stream lengths in the paleodrainage systems.

There are 5 paleodrainage profiles from which satisfactory downstream gradients of the paleodrainage systems can be obtained (Fig. 4), with downstream gradients in the range 0.08% to 0.44%. The lower gradient (0.08–0.1%) Cotagaita-top (Ct) and Villazon-S (VS) profiles are across aggradational surfaces. The Cotagaita-base (Cb), Puna-Yamparez (PY), and Villazon-N (VN) profiles are steeper (0.23–0.44%), and follow erosional surfaces. It is important to note that all these gradients are very insensitive to regional tilting about a north–south axis, because the drainage itself is predominantly in this direction (Fig. 4). In addition, because both north and south flowing profiles have been used, there will be no systematic bias as a consequence of a regional tilt about an east–west axis (Fig. 4). In the following analyses, we use the Cotagaita-base (Cb), Villazon-N (VN) and Puna-Yamparez (PY) erosional profiles (Figs. 4 and 7), with gradients in the range 0.2% to 0.5%, because these are likely to be hydrological analogues for the modern down-cutting rivers.

Table 2

Summary of paleosurface height and uplift estimates, using four different methods: (1) comparison of paleodrainage and modern river gradients; (2) projecting paleodrainage downstream to Late Miocene foreland; (3) projecting Subandean rivers upstream from Late Miocene foreland; (4) using maximum knickpoint heights above foreland

Drainage basin	h range[a] (m)	Modal h[a] (m)	Uplift[b] (m)
(1) *Uplift from river gradients*			
Rio Grande	0–2200	500	2080
Pilcomayo	0–2000	400	2240
San Juan del Oro	0–3600	350	2130
(2) *Projecting paleosurfaces downstream*			
Rio Grande	–	–	–
Pilcomayo	0–1500	500	2140
San Juan del Oro	0–1500	450	2030
(Cotagaita and Villazon)	0–1500	450	2710
(3) *Projecting Subandean rivers upstream*			
Rio Grande	0–1200	500	2080
Pilcomayo	–	–	–
San Juan del Oro	0–1200	600	1880
Knickpoint h_{max} (with ht of paleodrainage)[c] (m)	**Minimum uplift[d] (m)**	**Minimum uplift[e] (m)**	
(4) *Uplift from modern knickpoint heights*			
1070 (2960)	1890	1080	
1610 (2960)	1350	1080	
1880 (2800)	920	920	

[a] h = Elevation above foreland basin level; range values give the elevation range determined by each method, with modal values corresponding to the 'most likely' height estimate for each case. Two estimates are obtained for the 'project downstream' method for the Rio San Juan del Oro basin, as two paleodrainage profiles were sampled.

[b] All uplift estimates are calculated for the Eastern Cordillera at the eastern edge of the paleosurface remnants and are based on the assumption that the foreland basin level has remained constant.

[c] Maximum knickpoint height above foreland basin level in modern drainage basin, with height of paleosurface in brackets.

[d] Palaeosurface height − knickpoint height (h_{max}) for each river.

[e] Palaeosurface height − knickpoint height (h_{max}) of the Rio San Juan del Oro.

2.1.1. Comparison with modern river gradients

Various segments of the modern river system draining the Eastern Cordillera have gradients similar to those of the paleodrainage system. The segments are predominantly at the back of the Subandean zone, at elevations 100–500 m above the foreland basin level and significantly below the level of the paleosurfaces. For example, within the Rio Grande basin, a histogram of modern river elevations with slopes equivalent to those of the paleosurfaces has a modal value between ~100–600 m above the foreland basin level, though there is a long tail in the distribution, with a maximum elevation of ~2200 m (Fig. 5). Histograms for the Pilcomayo and San Juan del Oro drainage basins show a bimodal distribution, with lower elevations in the range 0 to 900 m above foreland level, and a higher elevations in the range 1800–2700 m (Fig. 5).

The lower modal height ranges could be taken as a minimum estimate of the original elevation of the paleodrainage systems, giving an upper bound estimate of rock uplift U_r. However, because there are knickpoints in the modern major trunk streams, the original elevation could be much higher (with corresponding less subsequent uplift U_r), corresponding to the higher elevation parts of the modern drainage system which also have similar gradients to the paleosurfaces.

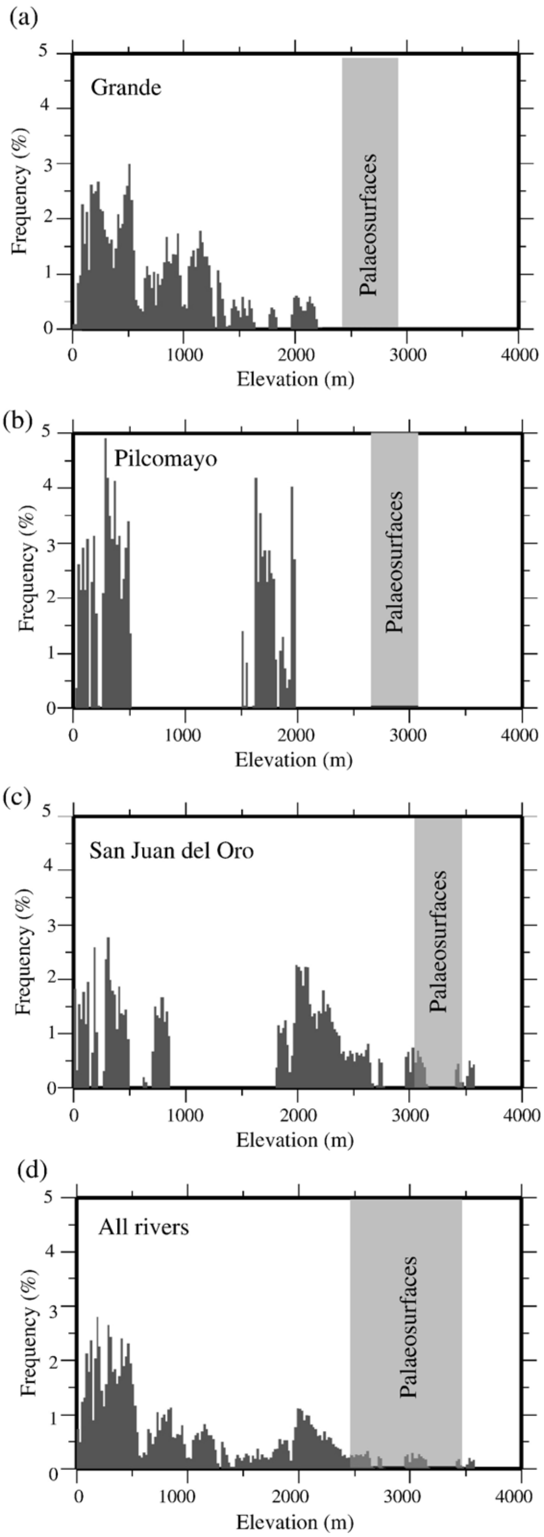

Fig. 5. Frequency histograms showing elevations of modern rivers with slopes between 0.2 and 0.5%, equivalent to those of the paleodrainage systems that flowed over the paleosurfaces. All heights are relative to the foreland basin level, and the grey region indicates the height of the palaeosurfaces remnants within each basin. (a) Frequency histogram for the Rio Grande basin (see Fig. 2). (b) Frequency histogram for the Pilcomayo basin (see Fig. 2). (c) Frequency histogram for the San Juan del Oro basin (see Fig. 2). (d) Frequency histogram for all rivers draining the eastern Bolivian Andes.

2.2. Projecting paleoriver profiles downstream of the paleosurfaces

Modern river profiles generally obey a simple empirical relationship, where the local river gradient or slope S, at any point along the profile, is [23,24]:

$$S = k_s A^{-\theta} \tag{1}$$

defined by constants k_s and θ, referred to as the steepness index and concavity, and the upstream area A of the catchment. Such a relationship is consistent with a number of bedrock incision models for river profiles. Thus, k_s and θ characterise the profile and can potentially be extracted from a paleodrainage system (Fig. 6). Given that the drainage basin geometries do not appear to have changed significantly since the abandonment of the paleosurfaces, we assign the along-stream drainage areas of the nearest rivers to the paleodrainage profiles. Once values of θ and k_s have been fitted, the profiles can be extrapolated downstream to determine the predicted height above base level of the paleodrainage in the foreland region (Fig. 7). Thus, the difference between this height and the present foreland elevation (corrected for any change in base level) is an estimate of U_r.

2.2.1. Original elevation of paleosurfaces

In all three profiles, θ is well constrained, with relatively low RMS values; the k_s value varies over an order of magnitude for the range of θ, but this variation is significantly less for the best fitting θ values. The original elevation of the paleodrainage is estimated using a Monte Carlo simulation to generate 10,000 triplets of k_s, θ, and along-stream length, given the uncertainties in these parameters. This way, frequency histograms of possible solutions for the three profiles have been generated (Fig. 8). These are all negatively skewed, with strong modal peaks at elevations of 300–500 m above the foreland basin level, with <10% of the total number of solutions above 1500 m. Only the results for the Puna-Yamparez (PY) profile have a tail reaching or exceeding the present paleosurface elevation, but this comprises only ~2% of the total solutions.

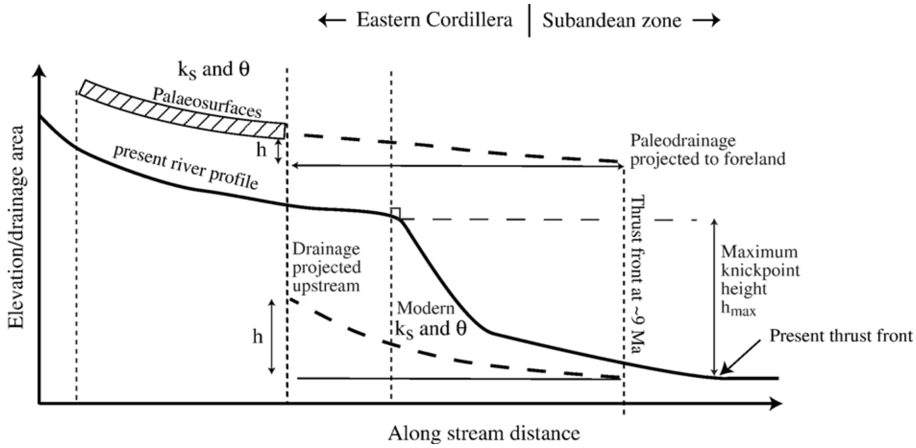

Fig. 6. Diagram illustrating three methods for estimating the original elevation of a paleodrainage system in the Eastern Cordillera in terms of its height h above the baselevel in the foreland. The first method involves extrapolating the paleodrainage profile downstream, using the mean concavity (θ) and steepness index (k_s) for the paleodrainage. The second method involves projecting modern Subandean river gradients upstream, using k_s and θ values for the present trunk streams, downstream of any major knickpoints. In both cases, drainage area and along-stream length data are taken from the nearest modern drainage system. The third method involves calculating the height of major knickpoints in the modern drainage, simply by subtracting the elevation of the knickpoint from the elevation of the base level, This yields a maximum knickpoint size, h_{max}.

2.3. Projecting modern river profiles upstream to the paleosurfaces

In this approach, we again make the assumption that the paleorivers downstream of the paleosurfaces had smooth profiles during the major phase of planation at ~12–~9 Ma. We determine the concavity and steepness indices (θ and k_s) of the present river profiles and make the assumption that these are the same as those for the paleorivers, and that the drainage area and along strike length also have not changed for the three major trunk streams. This way, we can project back the river profiles to the position of the most eastern paleosurfaces (Fig. 6). This approach has the advantage of not being dependent on measuring the present gradients across the paleosurfaces, but assumes instead that the river profile steepness indices and concavities have remained constant through time.

2.3.1. Original elevation of paleosurfaces

Barke [9] derived k_s and θ values for the rivers today that flow downstream of the paleosurface remnants (and therefore downstream of the major knickpoints) through the Subandean zone and into the foreland. The 'most likely' elevation of formation of the paleosurfaces is estimated from a Monte Carlo simulation, with 10,000 triplets of along-stream length, θ and k_s, given the maximum plausible ranges for these parameters (Fig. 9).

The distributions of height estimates for the Pilcomayo and San Juan del Oro paleodrainage basins are remarkably tight, despite the large standard deviations assigned to the parameters, with modal elevations in the range 500–700 m above the foreland basin level. Elevations >1500 m were only found ≪1% of the solutions. Given the tight distributions arising from the Monte Carlo modelling, these height estimates are relatively insensitive to the specific k_s, θ and along-stream length estimates.

The distribution for the Pilcomayo paleodrainage basin has high variance, with a potential modal value at ~1500 m. Heights above 2800 m for the Pilcomayo basin must reflect unrealistic parameter combinations that have exaggerated the elevation.

2.4. Knickpoints in paleodrainage systems

The previous estimates of uplift have been based on the assumption that the profiles of the rivers connecting the paleosurfaces to the foreland basin were smooth, described by unique values of the steepness index (k_s) and concavity (θ). In fact, the present trunk rivers have prominent knickpoints (Fig. 6). If knickpoints like these existed in the paleoriver profiles, then the amount of paleodrainage uplift would be greatly overestimated by the assumption of a smooth river profile.

Knickpoints are a consequence of local or rapid changes in a drainage system. For example, if the incision of the paleodrainage system was the result of a sudden drop in base level, or sudden uplift, or marked lithological contrasts in the drainage system, then a knickpoint will develop which may subsequently migrate upstream, progressively becoming more prominent [25]. The actual incision history for the paleosurfaces is not consistent with this scenario [9],

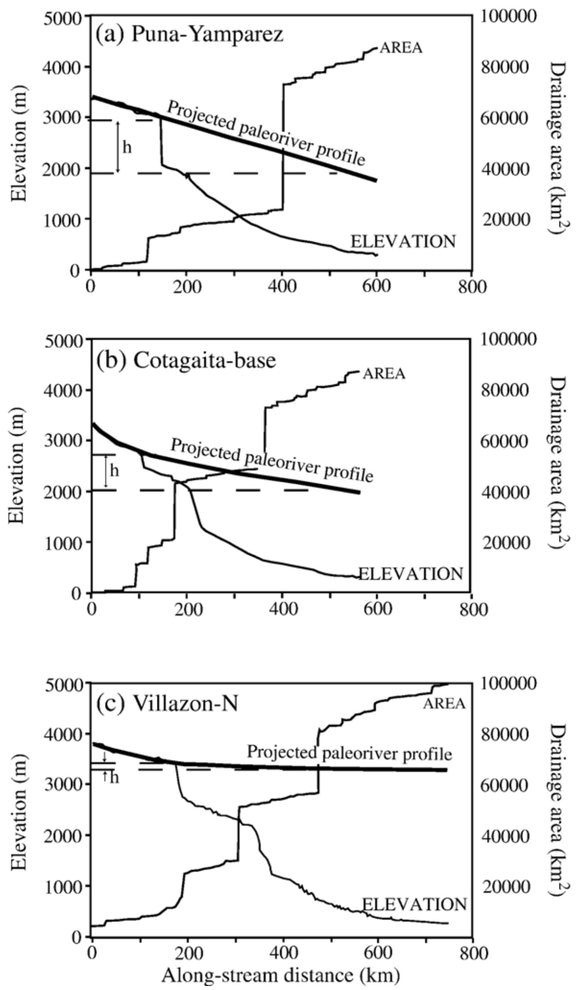

Fig. 7. Paleodrainage catchment area and elevation plotted against along-stream distance. Because of the similarity between the present drainage and paleodrainage systems in the Eastern Cordillera, the catchment areas and along-stream distances for the nearest major modern drainage are used, but assigned elevations of the paleosurfaces. By finding the best fit values of the steepness index and cavity for palaeoriver profiles in the vicinity of the paleosurfaces, the paleodrainage can be projected farther downstream towards the foreland (Fig. 6, see text for details of methodology). This way, the elevation *h* above the foreland, at which the paleosurfaces formed, can be estimated. (a) Projecting paleodrainage downstream for the Puna–Yamparez (PY) profile (see Fig. 4) in the Pilcomayo paleodrainage system. (b) Projecting paleodrainage downstream for the Cotagaita (Cb) profile (see Fig. 4) in the San Juan del Oro paleodrainage system. (c) Projecting paleodrainage downstream for the Villazon-N (VN) profile (see Fig. 4) in the San Juan del Oro paleodrainage system.

but it would predict that knickpoints in the paleodrainage system are no larger than those today in the modern river system. In addition, paleoclimatic indicators [13] (Paul Valdes personal communication) suggest that precipitation in the Eastern Cordillera has decreased in the last ~10 Ma, either as a consequence of global climate change or as a local response to uplift. In any case, such a decrease in precipitation would be expected to reduce run-off and erosion, resulting in steeper and more elevated stream profiles in uplifting regions. Therefore, whilst not generating knickpoints, steady uplift and a decrease in precipitation in the Eastern Cordillera are likely to have acted together to amplify any knickpoint. Lithological contrasts are unlikely to have changed, and, in any case, do not appear to exert an important control on the river profiles [9]. Thus, knickpoints observed in the present river profiles must be the largest that have existed since the formation of the paleosurfaces.

2.4.1. Knickpoint heights

Fig. 6 shows how knickpoint size can be quantified in the modern rivers. The simplest method is to take the river profile upstream of the knickpoint at the time of the paleodrainage system as horizontal, in which case the knickpoint height is the height of the top of the knickpoint (minus the elevation of the foreland basin). The approach gives an absolute maximum estimate of the height of the knickpoint, h_{max}, and hence a maximum estimate of the elevation of formation of the paleosurfaces, and is also independent of assumptions about the paleosurface drainage gradients.

The sizes of the knickpoints of the modern trunk streams are summarised in Table 2. Knickpoint height is greatest for the Rio San Juan del Oro, and decreases northwards. Uplift of the paleodrainage system is then estimated by simply subtracting the height of the knickpoint away from the height of the easternmost paleosurface remnants (assuming constant foreland basin elevation). If the knickpoint for the Rio San Juan del Oro is taken as the largest possible knickpoint at the time of formation of the paleosurfaces, then the minimum amount of uplift is ~1 km. If the knickpoints for each individual river are taken as the maximum knickpoints for each river system at ~12–~9 Ma, then the minimum amount of uplift for each drainage system varies from ~900 m for the Rio San Juan del Oro basin to ~1900 m for the Rio Grande basin.

3. Kinematic models of uplift in the Eastern Cordillera

Uplift will be a consequence of changes in either the thickness of the crust or lithospheric mantle. The large contrast between the crust (~2.7 gcm^{-3}) and mantle (~3.3 gcm^{-3}) densities, compared to the density difference between lithospheric and asthenospheric mantle (0.04–0.07 gcm^{-3}), makes crustal thickening a powerful mechanism of uplift. Thus, 1 km of surface uplift requires ~5.5 km of crustal thickening, or 55–

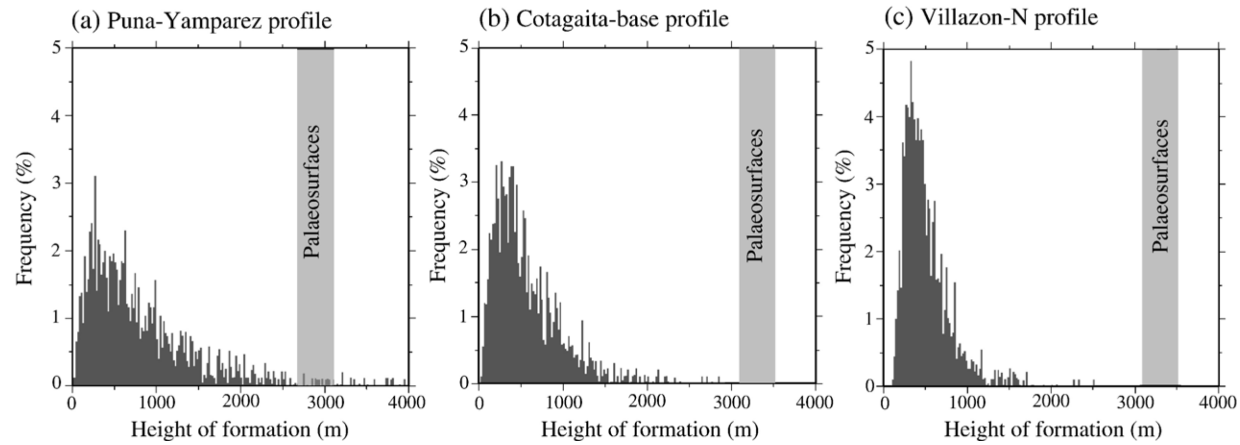

Fig. 8. Frequency histograms showing the most likely height of formation of the palaeosurfaces, based on projecting palaeosurface gradients downstream, using the results of Monte Carlo restart analysis for 10,000 combinations of θ, k_s within their plausible ranges. This analysis suggests that the most likely height at which the paleosurfaces formed is approximately 400–500 m above the foreland basin level. (a) Frequency histogram for the Puna–Yamparez (PY) profile in the Pilcomayo basin (see Figs. 2 and 4). (b) Frequency histogram for the Cotagaita-base (Cb) profile in the San Juan del Oro basin (see Figs. 2 and 4). (c) Frequency histogram for the Villazon-N (VN) profile in the San Juan del Oro basin (see Figs. 2 and 4).

110 km of lithospheric mantle thinning. A wealth of structural, gravity and seismic evidence, in addition to the lack of any Cenozoic volcanism, indicate an 'old and cold' lithosphere beneath most of the Eastern Cordillera, with shortening on its eastern margin, in the Subandean zone, accommodated in a thin wedge, above a west dipping basal decollement at depths between 5 to 15 km [9,26–34].

The easternmost remnants of the Late Miocene paleodrainage systems analysed in this study lie only ~50 km from the western edge of the Subandean thin-skinned fold and thrust belt. This proximity strongly suggests that shortening in the Subandean zone is linked to uplift farther west [32,33], in the Eastern Cordillera. In this case, the time scale for uplift of the Eastern Cordillera is essentially the same as that for shortening in the Subandean zone, continuing up to the present, though not necessarily at a constant rate. In fact, the relatively constant rate of incision of rivers in the Eastern Cordillera since ~9 Ma, between 100 and 200 m/Ma suggests uplift has preceded at a similarly uniform rate [9]. In addition, the Pislepampa flora in the Eastern Cordillera suggests significant uplift since 6–7 Ma [12,13].

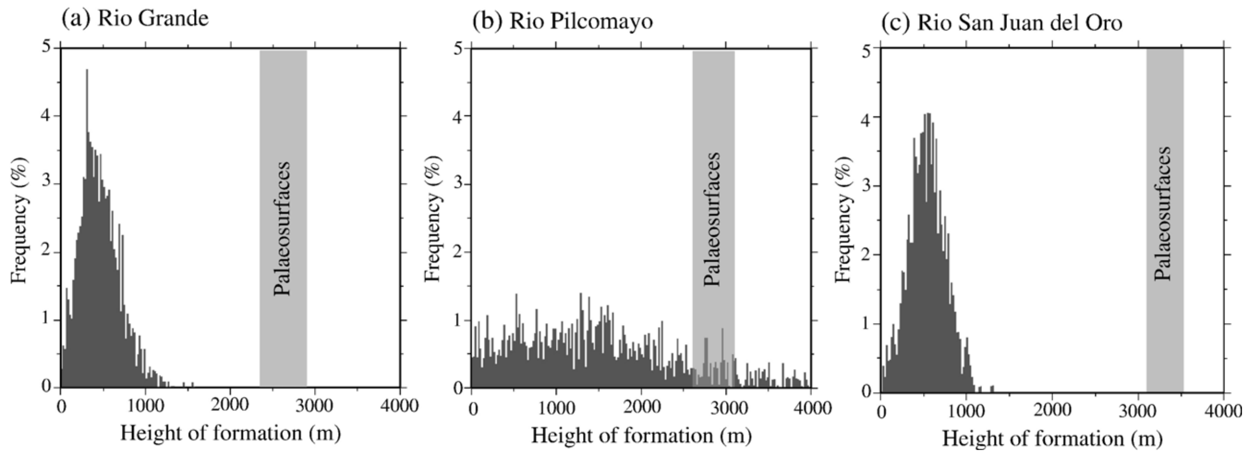

Fig. 9. Frequency histograms showing the most likely height of formation of the palaeosurfaces, based on projecting present Subandean gradients upstream (Fig. 6), using the results of Monte Carlo restart analysis for 10,000 combinations of θ, k_s within their plausible ranges. This analysis suggests that the most likely height at which the palaeosurfaces formed is approximately 500 m above the foreland basin level. (a) Frequency histogram for the Rio Grande basin (see Fig. 2). (b) Frequency histogram for the Pilcomayo basin (see Fig. 2). (c) Frequency histogram for the San Juan del Oro basin (see Fig. 2).

3.1. Uplift of the Eastern Cordillera by sliding up a thrust ramp

Rock uplift (U_r) will depend on the amount of crustal thickening, erosion (E), and also the degree of isostatic compensation. We can consider two end-member models for crustal thickening beneath the paleosurfaces, either involving displacement on a major low angle fault, or pervasive ductile lower crustal flow (discussed in Section 3.2). Thus, a very simple model for uplift in the Eastern Cordillera is a rigid block sliding up a thrust ramp in the west dipping basal thrust (or ductile shear zone) above the flexurally strong Brazilian Shield (Fig. 10a). Note that displacement (D) on the ramp will only lead to crustal thickening if the dip of the ramp (ϕ) is greater than that of the Moho (α), so that the ramp makes an angle with the Moho (referred to as the crustal cut-off angle, ϕ–α). As we are only considering uniform uplift of the paleosurfaces, it is sufficient for our purposes to consider average values of these factors in a simple 1-D kinematic model [35]:

$$U_r \approx \frac{D\tan(\phi-\alpha)}{k_{\mathrm{ic}}} + \frac{(k_{\mathrm{ic}}-1)}{k_{\mathrm{ic}}}E \qquad (2)$$

where k_{ic} is a measure of the degree of isostatic compensation [7,35]. For the case of simple Airy isostasy, $k_{\mathrm{ic}}=\rho_m/(\rho_c-\rho_m)$, whereas $k_{\mathrm{ic}}=1$ for no compensation. We can use this model in two ways. Firstly, we can use the estimates of uplift to constrain the crustal cut-off angle

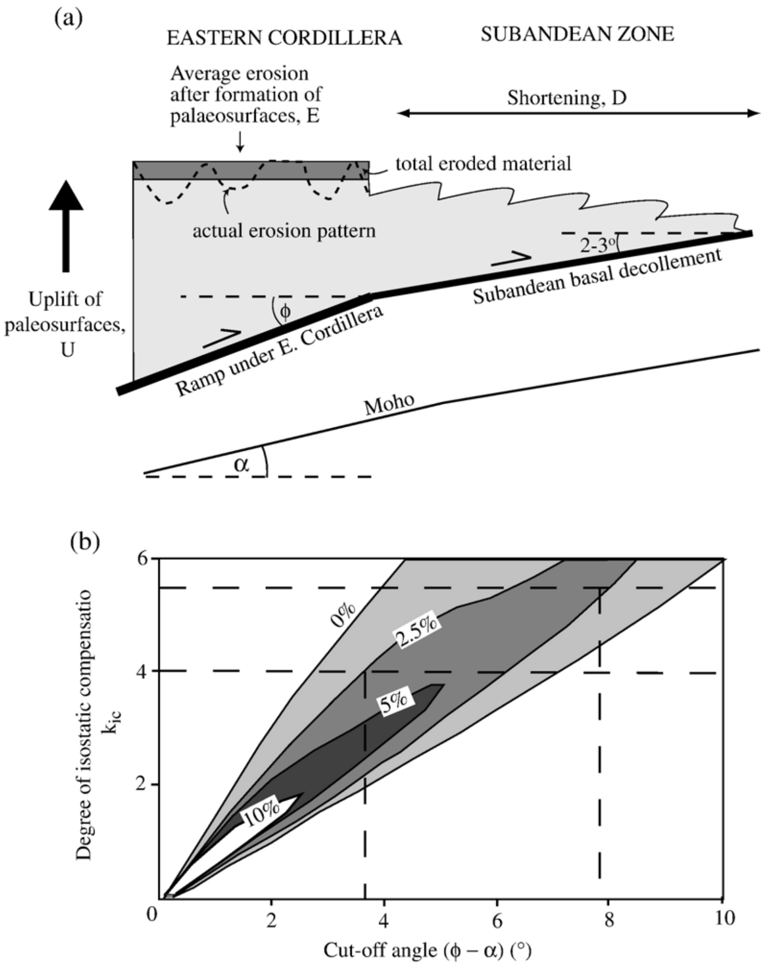

Fig. 10. (a) Kinematic model for the uplift of the palaeosurfaces as a consequence of sliding up a thrust ramp in the basal decollement (with dip ϕ), accommodated by shortening in the Subandean zone. Uplift U, is a function of the crustal cut-off angle ($\phi-\alpha$, where α is the dip of the underlying Moho), as well as the amount of shortening in the Subandean zone D, the degree of isostatic compensation (defined by the parameter k_{ic}), and the average amount of erosion (E) since formation of the palaeosurfaces (see text). (b) Frequency plot, showing the possible combinations of k_{ic} and crustal cut-off angle ($\phi-\alpha$) calculated for 10,000 random combinations of U, D and E within their plausible ranges. The plausible value of k_{ic} is bracketed between 4.0 and 5.5 for the Eastern Cordillera (see text), leading to corresponding best fit values of $\phi-\alpha$ between 3.8° and 7.8°.

(ϕ–α). And secondly, we can look for independent confirmation of the uplift estimate by comparing the so derived dip with the structure in the region. Note that the ramp model requires the entire region of paleosurface remnants to have risen up the ramp, and so the ramp must extend at least as far west of the westernmost remnants as the displacement distance. The lack of tilting of the paleosurfaces constrains the ramp to underlie the easternmost paleosurface remnants.

3.1.1. Estimates of E and D

The amount of incision into the paleosurfaces is greatest in the north (north of 19°S) and decreases towards the south. Taking an average elevation of the paleosurfaces of 3250 m, the 90 m digitital elevation model can be used to calculate an average amount of erosion into the paleosurfaces of 230 ± 90 m [9]. In our simple model, the displacement on the ramp will equal the amount of shortening in the Subandean zone. Barke [9] used field mapping combined with an interpretation of oil company seismic reflection profiles to construct two balanced cross-sections through the Subandean zone at ~20°S and between 64.25°W and 63°W (Figs. 1 and 11). By varying assumptions about the detachment zones in the stratigraphy, as well as local fault cut-off angles, minimum and maximum shortening estimates vary between 62 km and 85 km (73.5 ± 11.5 km). McQuarrie [33] estimated ~110 km of shortening for essentially the same transect, using measurements from her published cross-section (though 67 km is quoted in the text for the same cross-section), whereas Dunn et al. [34] estimated ~100 km shortening across the Subandean zone ~200 km farther south at ~22°S.

3.1.2. Dip of the thrust ramp

Fig. 10b shows the relation between the crustal cut-off angle (ϕ–α) and degree isostatic compensation k_{ic}, based on Monte Carlo solutions of Eq. (2) with 10,000 random triplets of D (taken from [9]), U_r, E within their uncertainty limits. This plot can be used to estimate the most probable values of the cut-off angle, because we can place limits on the expected value of k_{ic} in the Eastern Cordillera. Thus, if the crust is weak, with simple Airy isostasy, then for average crustal and mantle densities of 2.7 g/cm^3 and 3.3 g/cm^3 appropriate for the Bolivian Andes from seismic studies [36], the maximum value of k_{ic} is 5.5. A value for k_{ic} of ~4 may be estimated from balanced cross-sections of the Subandean fold and thrust belt [9], but the effective

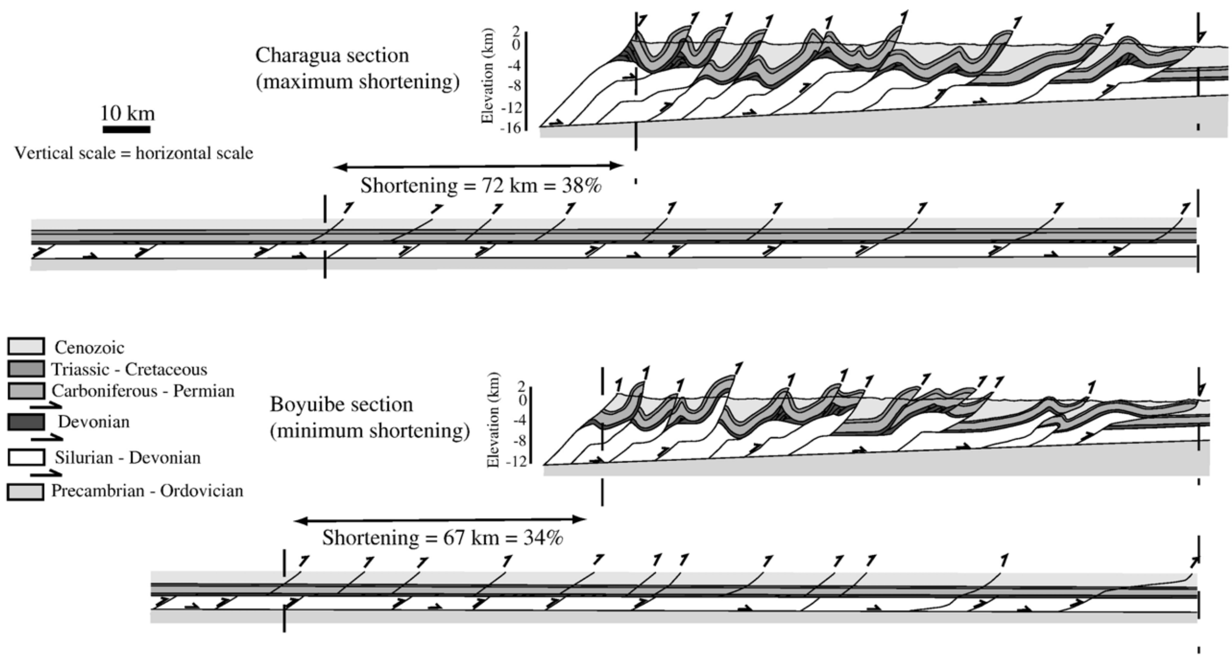

Fig. 11. Shortening estimates in the Subandean zone on the eastern margin of the Bolivian Andes between ~20°S and ~20.5°S, after [9]. Balanced east–west cross-sections (deformed and restored) along the Charagua (~20°S) and Boyuibe (~20.5°S) transects are based on field data and oil company seismic data (close to the line of cross-section in Fig. 1). The sections comprise a triangular prism of deformed Silurian to Cenozoic sequence, resting above a basal decollement on undeformed Ordovician to Pre-Cambrian basement. Major detachments follow stratigraphically controlled zones of weakness. The Charagua section has been constructed to maximise shortening, by assuming low thrust cut-off angles and a more steeply dipping basal decollement, whereas the Boyuibe section has been constructed to minimise shortening, by assuming larger thrust cut-off angles and a shallower decollement. The full range of possible sections suggest 73.5 ± 11.5 km of shortening at the level of the Mesozoic sequences (see text).

k_{ic} may be even lower at the relatively short length scales of thrust displacement (<100 km). In addition, k_{ic} would be expected to increase towards the west, sympathetic with a decrease in the flexural rigidity of the underlying lithosphere [27,31,37].

Fig. 10b constrains the most probable value of crustal cut-off angle in the range 3.8° to 7.8°. McQuarrie's and Dunn et al's [33,34] higher estimates of shortening *D* place the cut-off angle at the lower end of this range. In any case, for a Moho dipping at 2° to 8° [36], the predicted dip of the basal thrust is 6° to 16°. However, if k_{ic} decreases up the ramp as a consequence of the flexural rigidity of the underthrust Brazilian Shield, or is significantly lower at the lengths scales of thrust displacement, the dip of the Moho can be virtually neglected, and the ramp could flatten out significantly toward the east. So, the dip of the ramp is best constrained between 4° and 16°W, and between 2° and 14° steeper than the basal decollement beneath the Subandean zone, and remarkably similar to thrust geometries in published balanced cross-sections [32,33,38] and the expected flexural curvature of the underlying lithosphere [27,31,37]. In addition, Allmendinger and Zapata [39] imaged a major thrust ramp dipping at 20–40°W beneath the southernmost paleosurface remnants. Though this ramp is steeper than that required in our simple kinematic model, and is most likely inactive, it shows that there has been significant ramping of the basal decollement beneath the paleodrainage systems.

3.2. Uplift of the Eastern Cordillera by lower crustal flow

The 24–1.5 Ma Los Frailes volcanic complex and older intrusions and stocks [9,40] straddles the ~110 km wide region on the western margin of the Eastern Cordillera, between the paleodrainage remnants and the Altiplano (Fig. 12). Here, the youngest ~2 Ma eruptions are exposed in the central part of the complex, with older 12–6 Ma eruptions outcropping round the edges, with even

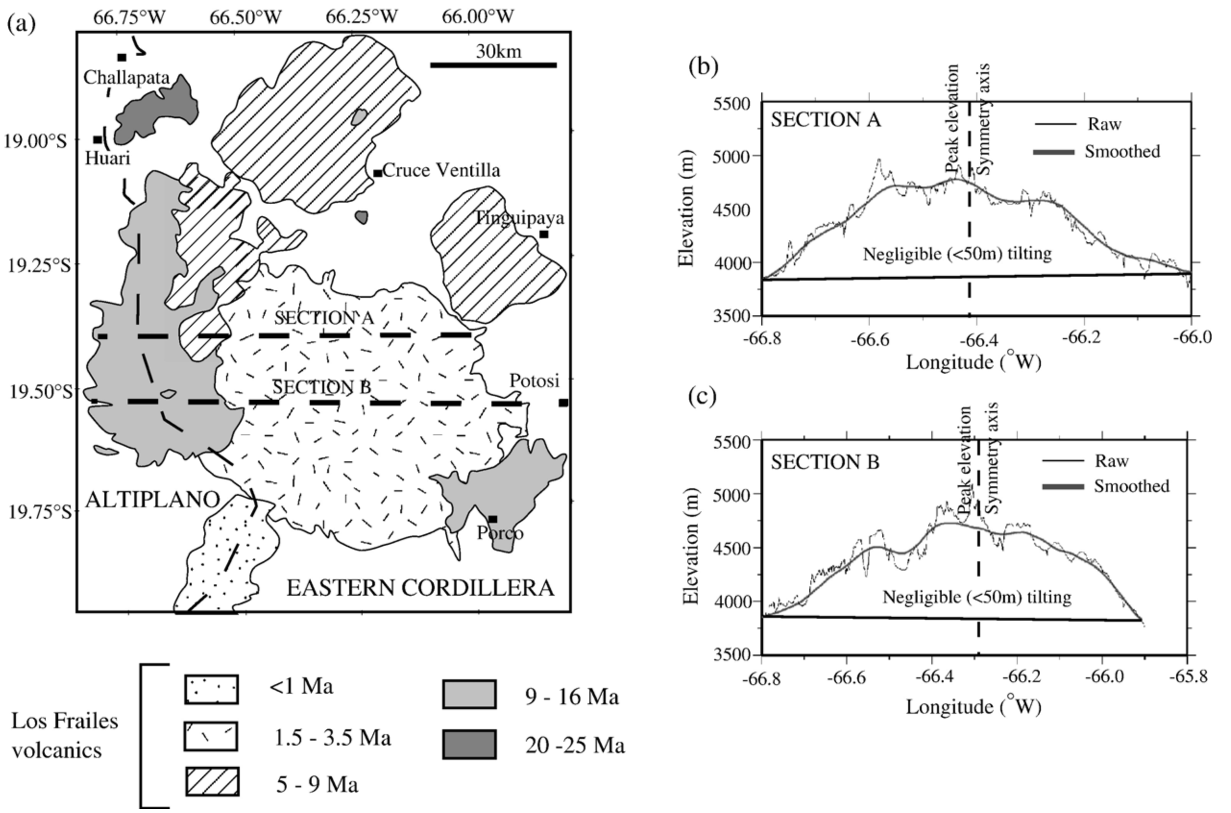

Fig. 12. Topographic profiles across the Los Frailes ignimbrite complex, on the western margin of the Eastern Cordillera, just west of the paleosurface remnants. (a) Geological map of the Los Frailes complex after [9]), showing the lines of section. Note that the oldest flows and intrusions outcrop on the margins of the complex, with the youngest in the central part, burying the older ones. This way, volcanism has built up a broad dome. (b) and (c) Topographic profiles across the complex. Thin line is raw profile, thicker line is a profile taken through applying a mean box filter to the topography, with size of 9 km × 9 km. The observed morphology is approximately symmetric; the change in elevation of the base of the flows across the complex is only ~50 m. This morphology suggests that the volcanics were erupted onto a near horizontal surface, with negligible tilting across the volcanic complex.

older pre-Los Frailes 24–13 Ma dacitic stocks and domes on the fringes, and so there has been no systematic migration of volcanic activity. Most likely, the younger ignimbrite flows have covered older ones, building up an overall broad dome-like structure [40].

Topographic cross-sections through the centre of the Los Frailes complex (Fig. 12) clearly show that it is essentially symmetrical, and that the difference in height between the basal flows at opposite sides is <50 m. This morphology is most easily explained if there has been negligible differential uplift on the western margin of the Eastern Cordillera in this region (<0.03°), and the possible differential uplift is much less than the error associated with the uplift estimates of the paleosurfaces themselves. Therefore, the best estimate of uplift here, since ~10 Ma, is equal to that of the paleosurfaces, at 1705±650 m. The relatively small amount of erosion of these volcanics suggests that rock uplift is approximately equal to surface uplift.

The mechanism of uplift of the Los Frailes volcanic complex could also be a consequence of sliding up a continuation of the ramp beneath the Eastern Cordillera farther east. However, the presence of extensive rhyolitic and dacitic magmatism since ~24 Ma, with major ignimbrite eruptions between ~12 and ~2 Ma, as well as very high heat flow, and evidence for active mantle melting in geothermal emissions [9,15,40,41,43,44] are all signs of a weak lithosphere, with temperatures at >10 km depth sufficiently high for extensive ductile flow (~80 mWm^{-2} or ~30 °C/km, [43]). This suggests a piston model [7,17,45], where flow is the result of the rigid lower crust beneath the basal decollement in the Subandean zone and Eastern Cordillera pushing its way into the ductile lower crust beneath the regions farther west (Fig. 13). This will result in shortening in the lower crust equivalent to the upper crustal shortening in the Subandean zone.

The piston model yields a surface uplift U_s simply given by $\Delta lC/(k_{ic}l_f)$, where C is the thickness of the piston pushing into the ductile lower crust (25±5 km), Δl is equal to the shortening in the Subandean zone, l_f is the width of the shortening zone, and k_{ic} is as before. If l_f is taken as the width of the region covering the western margin of the Eastern Cordillera and the eastern margin of the Altiplano (~150 km), then surface uplift will be ~2.3 km, using Barke's [9] estimates of Subandean shortening. But if the zone of lower crustal flow extends right across the Altiplano and volcanic arc, into the

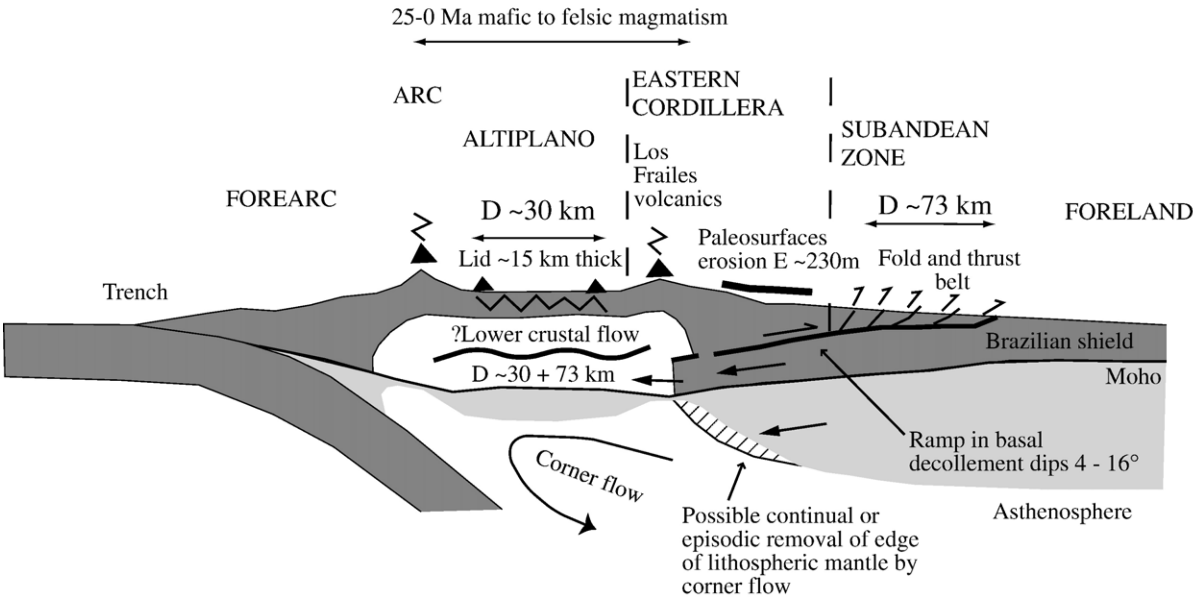

Fig. 13. Summary cartoon cross-section (see Fig. 1) illustrating a model for crustal shortening, thickening and uplift in the Eastern Cordillera since ~10 Ma. Crustal and lithospheric structure modified from [29,36,49]. Shortening (D ~73 km) in the brittle upper crust has been focussed in the Subandean zone, with some shortening (D ~30 km) in the Altiplano. Erosion and sliding up a ramp in the basal decollement, dipping at 4°–16°W, produces ~2 km of rock uplift in the eastern part of the Eastern Cordillera. Underthrusting of the Brazilian Shield acts like a piston, transferring the shortening to the lower ductile crust farther west, driving lower crustal thickening and surface uplift in these regions, with some brittle crustal shortening. The virtually continuous history since ~25 Ma of crustal melting, and several episodes of mafic volcanism with a shallow mantle melt source (50–90 km), right across the high Andes, all suggest that the lithosphere here has been thin on this time scale. However, as thicker lithospheric mantle beneath the Eastern Cordillera is transported westward, it may be continually or episodically removed as it comes closer to the asthenospheric corner flow; episodic removal could trigger local uplift of the overlying crust (see text).

Western Cordillera much farther west, then $l_f \sim 375$, and U_s is 0.9 km. McQuarrie's [31] shortening estimates require even larger uplift between 1.3 and 3.3 km. The effects of erosion, as well as magmatic addition to the crust, taking account of the likely volume at depth, will further increase this uplift by ≤ 300 m [9].

If the region of ductile flow extends farther east, beneath the paleodrainage systems themselves, then uplift here may also be a consequence of distributed crustal thickening at depth (rather than displacement on a localised ramp or shear zone), as suggested by [39]. In this case, the thickness of the piston is likely to be closer to that of the underthrust Brazilian Shield beneath the Subandean zone (~35 km), and predicted rock uplift will be >1.5, depending on whether the ductile flow only occurs beneath the Eastern Cordillera or extends right across the high Andes.

All these estimates of uplift are remarkably consistent with the observed 1.7 ± 0.7 km of rock uplift for the paleodrainage systems, and so lower crustal flow must be considered as a plausible mechanism of uplift.

4. Discussion

An important question is whether the mechanisms described above also apply to the Altiplano and volcanic arc. Magmatic addition is likely to be a significant mechanism of Cenozoic crustal thickening beneath the volcanic arc, accounting for up to 40% of the local crustal thickening beneath the volcanic arc [8,46]. Thinning of the lithospheric mantle has been long proposed as a mechanism of uplift for the Altiplano [8,42]. Indeed, new estimates of the uplift history of the northern Bolivian Altiplano (Fig. 1) from oxygen isotope data, which suggest 2.5 to 3.5 km of rock uplift between ~10 and 6.8 Ma, and essentially no uplift thereafter, have been taken as strong evidence for this thinning [2]. The amount of uplift would require rapid removal of 140 to 385 km of lithospheric mantle (for a 0.04–0.07 gcm^{-3} mantle density contrast between the lithosphere and asthenosphere). Alternatively, it could be explained by delamination of 35 to 45 km of eclogitic crust (~3.55 gcm^{-3}), or some combination of eclogite and mantle [2]. These scenarios do not fit easily with the known geological evolution of the Bolivian Andes. It seems implausible to us that the crust beneath the Altiplano at ~10 Ma was ~100 km thick, with the subsequent detachment of a ~40 km thick basal layer of eclogite by ~6.8 Ma. Certainly, such a thick eclogite layer could not be the result of Cenozoic (or Mesozoic) mafic magmatism behind the arc, as melt thicknesses at depth would not be expected to be more than a few kilometres, given the volume of surface eruptions [6]. In addition, seismic tomography shows that mantle lithosphere still occurs beneath the Altiplano [29].

An important constraint on the lithospheric structure is the long lived history of mafic, intermediate and acidic magmatism, right across the high Andes over the last ~25 Ma (Figs. 1 and 12) [8,46,47]. It seems likely that mantle melts introduced at depth are the heat source for crustal melting [8,29,42]; there have been at least three episodes of mafic volcanism in the northern and central Altiplano, with significant phases at 25–22 Ma [8,15] and 13–11 Ma [41] (Fig. 1), with minor eruptions between 5–0 Ma [8,15], as well as an elevated mantle helium-3 anomaly today in geothermal emissions right across the high Andes [42]. The Pleistocene and 25–22 Ma basic volcanics have a similar geochemistry [48], with the characteristic trace element signature of a shallow mantle melt source region extending from a depth of 50 km to 90 km (Dan McKenzie, pers. comm., L. Hoke and S. Lamb, Cenozoic behind-arc volcanism in the Bolivian Andes, South America: implications for mantle melt generation and lithospheric structure, manuscript submitted to the Journal of the Geological Society of London, June 2006). This would imply a thin mantle part of the lithosphere, a few tens of kilometres thick at most, throughout this period, with no obvious magmatic evidence for a significant change in the regional thermal structure and thickness of the lithosphere between ~10 and 6.8 Ma, coinciding with uplift of the Altiplano. Also, the subducted slab beneath the volcanic arc is at ~110 km depth, and so unless the arc melt source in the Miocene was significantly deeper than that for volcanic arcs today, there is little room for thick Miocene mantle lithosphere here as well.

None-the-less, the westward underthrusting of thick lithosphere beneath the Eastern Cordillera might be expected to result in a westward migration of the edge of the zone of thin lithosphere (Fig. 13). However, the relatively constant position of the eastern limit of Neogene magmatism (Fig. 1), clearly evident in the Los Frailes volcanic complex (Figs. 1, 12, 13), suggests that this has not happened by more than a few tens of kilometres, and much less than the amount of shortening in the Eastern Cordillera and Subandean zone. This suggests that westward underthrusting of mantle lithosphere is counteracted by some form of lithospheric removal, most likely triggered by interaction with the asthenospheric corner flow (Fig. 13). Continual removal will have no effect on surface uplift, because the lithospheric structure will remain constant, albeit with a marked step downwards to the east, where it thickens (Fig. 13). However, episodic removal on its own will give rise to a see-saw pattern of local uplift and subsidence, in which underthrusting of dense lithosphere, replacing buoyant asthensophere, will cause subsidence of the overlying crust, and subsequent removal will trigger uplift. For a typical average rate of underthrusting of 7.5 mm/yr, 40–75 km of underthrust lithosphere would need to be removed every 5 to 10 Ma, triggering <1 km local uplift events (assuming ~100 km thick mantle lithosphere and 10 km of eclogitic lower crust, consistent with the crustal structure beneath the Eastern Cordillera [49], followed by a similar amount of subsidence.

We note also the following. (1) The onset of Late Miocene uplift in the northern Altiplano coincides with an intense phase of shortening, and presumably crustal thickening, in the same region [2,8,9,12], starting at ~9.5 Ma but certainly continuing after ~5 Ma, up to 2.7 Ma and possibly younger, because the sequences studied by Garzione et al. [2] lie in the hanging wall of a major fold and thrust structure that also deforms ~5 Ma and younger volcanics and sediments [8]. (2) It is easy to show that the expected homogeneous thickening of the crust (~60 km thick) beneath the northern Altiplano, as a consequence of the observed ~30 km to ~40 km of crustal shortening since ~9.5 Ma [8,33], would result in >1 km of surface uplift, which, with the addition of lower crustal squeezing to accommodate shortening in the thin-skinned Subandean fold and thrust belt, could easily be increased to >2 km, though some uplift would have continued beyond Garzione et al's cut-off date of ~6.8 Ma [2]. (3) The Altiplano appears to have remained mainly an internal drainage basin since 25 Ma, and so it cannot have been on average higher than the western margin of the Eastern Cordillera or volcanic arc during the Neogene, unless the internal drainage system was breached. (4) The Altiplano is a vast region with numerous sub-basins, extending for >1000 km along its length, and so the mechanism and history of uplift may vary from place to place, for example between parts that have acted as sedimentary basins and those that are locally undergoing deformation and erosion.

Whatever the details of the Late Cenozoic history of uplift for the Bolivian Andes, it seems clear that crustal thickening has played an important role, at least in the Eastern Cordillera. Lithospheric thinning may be significant too, although it is very hard to account for more than 0.5 to 1 km of regional uplift by this mechanism, because this would involve the rapid removal of much more than a few tens of kilometres of lithospheric mantle, together with more than 10 km or so of eclogitised crust across the entire high Andes, in a region extending for ~400 km in width, and >1000 km in length, where magmatic evidence points to a thin lithosphere since ~25 Ma.

5. Conclusions

The morphology of well preserved paleosurfaces, defining Late Miocene paleodrainage systems is used to estimate Late Cenozoic rock uplift of the Eastern Cordillera in the Bolivian Andes. Using four different methods, the best estimate of uplift since 12–9 Ma is 1705±695 m. During the same period there has been on average 230±90 m of erosion in the region. The lack of tilting in the regions farther west strongly suggest that rock uplift of the paleodrainage systems also extends at least to the western margin of the Eastern Cordillera, ~100 km farther west.

The estimated uplift of the Eastern Cordillera easily satisfies the kinematic requirement that 62–110 km of thin-skinned shortening in the Subandean zone is balanced by shortening at depth farther west. Uplift in the Eastern Cordillera is explained by sliding up a ramp in the west dipping basal decollement, dipping at 4° to 16°W. Uplift of the western margin of the Eastern Cordillera can be explained in terms of ductile flow in the lower crust which accommodates underthrusting of the rigid lower crust, farther east, resulting in ~2 km of rock uplift. The good agreement in these simple models suggest that crustal thickening is an important mechanism of Late Cenozoic surface uplift in the Bolivian Andes.

Acknowledgements

This work was supported by grants from NERC, Royal Society, and EU, and was carried out during a studentship (RB) tied to a NERC research grant held by SL. This work would not have been possible without the encouragement of Barry Parsons, who was instrumental in organising the early availability of the SRTM digital topographic data. We would like to especially thank Estela Minaya, Directora of the Observatorio San Calixto, for her help and collaboration. We also thank Gareth Funning, James and Alfredo Quisberth, and Maximo Paredes for all their help in the field.

References

[1] P. Molnar, P. England, J. Martinod, Mantle dynamics, uplift of the Tibetan Plateau, and the Indian monsoon, Rev. Geophys. 31 (1993) 357–396.

[2] C.N. Garzione, P. Molnar, J.C. Libarkin, B.J. MacFaden, Rapid Late Miocene rise of Bolivian Altiplano: evidence for removal of mantle lithosphere, Earth Planet. Sci. Lett. 241 (2006) 543–556.

[3] J. Kley, C.R. Monaldi, Tectonic shortening and crustal thickening in the Central Andes: how good is the correlation? Geology 26 (1998) 723–726.

[4] D. Hindle, J. Kley, O. Oncken, S. Sobolev, Crustal balance and crustal flux from shortening estimates in the Central Andes, Earth Planet. Sci. Lett. 230 (2005) 113–124.
[5] R.W. Allmendinger, B.L. Isacks, T.E. Jordan, S.M. Kay, The evolution of the Altiplano–Puna plateau of the Central Andes, Annu. Rev. Earth Planet. Sci. 25 (1997) 139–174.
[6] T.E. Jordan, J.H. Reynolds III, J.P. Erikson, Variability in age of initial shortening and uplift in the Central Andes, 16–33°30′S, in: W. Ruddiman (Ed.), Tectonic Uplift and Climate Change, Plenum Publishing, New York, 1997, 41 pp.
[7] T.L. Gubbels, B.L. Isacks, E. Farrar, High-level surfaces, plateau uplift, and foreland development, Bolivian Central Andes, Geology 21 (1993) 695–698.
[8] S.H. Lamb, L. Hoke, Origin of the high plateau in the Central Andes, Bolivia, South America, Tectonics 16 (1997) 264–623.
[9] R.M.D. Barke, Late Cenozoic tectonic and topographic evolution of the Bolivian Andes, DPhil Thesis, Oxford University (2004).
[10] J.T. Singewald, E.W. Berry, The geology of the Corocoro copper district of Bolivia, John Hopkins University Studies in Geology, vol. 1, 1922, pp. 1–117.
[11] E.W. Berry, The fossil flora of Potosi, Bolivia, John Hopkins University Studies in Geology, vol. 13, 1939, pp. 1–67.
[12] K.M. Gregory-Wodzicki, Uplift history of the Central and Northern Andes: a review, Bull. Geol. Soc. Am. 112 (7) (2000) 1091–1105.
[13] A. Graham, K.M. Gregory-Wodzicki, K.L. Wright, Studies in neotropical paleobotany. XV. A Mio-Pliocene palynoflora from the Eastern Cordillera, Bolivia: implications for the uplift history of the Central Andes, Am. J. Bot. 146 (3) (2001) 813–826.
[14] L. Kennan, S.H. Lamb, L. Hoke, High-altitude palaeosurfaces in the Bolivian Andes: evidence for Late Cenozoic surface uplift, Geol. Soc. London, Spec. Publ. 120 (1997) 307–323.
[15] L. Kennan, S.H. Lamb, C. Rundle, K–Ar dates from the Altiplano and Cordillera Oriental of Bolivia: implications for Cenozoic stratigraphy and tectonics, J. South Am. Earth Sci. 8 (2) (1995) 163–186.
[16] T.T. Cladouhos, R.W. Allmendinger, B. Coira, E. Farrar, Late Cenozoic deformation in the Central Andes: fault kinematics from the northern Puna, northwest Argentina and southwest Bolivia, J. South Am. Earth Sci. 7 (1994) 209–228.
[17] S.H. Lamb, Active deformation in the Bolivian Andes, South America, J. Geophys. Res. 105 (B11) (2000) 25627–25653.
[18] S.H. Lamb, L. Hoke, L. Kennan, J. Dewey, Cenozoic evolution of the Central Andes in northern Chile and Bolivia, in: J.-P. Burg, M. Ford (Eds.), Orogens Through Time, Spec Publ. Geol. Soc. Lond., vol. 121, 1997, pp. 237–264.
[19] L. Echavarria, R. Hernandez, R. Allmendinger, J. Reynolds, Subandean thrust and fold belt of northwestern Argentina, Geometry and timing of the Andean evolution, Am. Assoc. Pet. Geol. Bull. 87 (6) (2003) 965–985.
[20] L.G. Marshall, T. Sempere, M. Gayet, The Petaca (Late Oligocene–Middle Miocene) and Yecua (Late Miocene) Formations of the Subandean–Chaco basin, Bolivia, and their tectonic significance, Doc. Lab. Geol. Lyon 125 (1993) 291–301.
[21] J.H. Reynolds, C.I. Galli, R.M. Hernandez, B.D. Idleman, J.M. Kotila, R.V. Hilliard, C.W. Naeser, Middle Miocene tectonic development of the transition zone, Salta Province, northwest Argentina; magnetic stratigraphy from the Metan Subgroup, Sierra de Gonzalez, Bull. Geol. Soc. Am. 112 (2000) 1736–1751.
[22] C.E. Uba, C. Heubeck, C. Hulka, Facies analysis and basin architecture of the Neogene Subandean synorogenic wedge, southern Bolivia, Sediment. Geol. 180 (2005) 91–123.
[23] J.J. Flint, Stream gradient as a function of order, magnitude, and discharge, Water Resour. Res. 10 (1974) 969–973.
[24] D.G. Tarboton, R.L. Bras, I. Rodriguez-Iturbe, Scaling and elevation in river networks, Water Resour. Res. 25 (9) (1989) 2037–2051.
[25] K.X. Whipple, G.E. Tucker, Implications of sediment-flux-dependent river incision models for landsape evolution, J. Geophys. Res. 107 (B2) (2002), doi:10.1029/2000JB000044.
[26] H. Lyon-Caen, P. Molnar, G. Suarez, Gravity anomalies and flexure of the Brazilian shield beneath the Bolivian Andes, Earth Planet. Sci. Lett. 75 (1985) 81–92.
[27] A. Watts, S.H. Lamb, J. Fairhead, J.F. Dewey, Lithospheric flexure and bending of the Central Andes, Earth Planet. Sci. Lett. 134 (1995) 9–21.
[28] P. Baby, P. Rochat, G. Mascle, G. Herail, Neogene shortening contribution to crustal thickening in the back arc of the Central Andes, Geology 25 (10) (1997) 883–886.
[29] S.C. Myers, S. Beck, G. Zandt, T. Wallace, Lithospheric-scale structure across the Bolivian Andes from tomographic images of velocity and attenuation for P and S waves, J. Geophys. Res. 103 (1998) 21233–21252.
[30] D. Whitman, B.L. Isacks, J.-L. Chatelain, J.-M. Chiu, A. Perez, Attenuation of high frequency seismic waves beneath the Central Andean plateau, J. Geophys. Res. 97 (1992) 19,929–19,947.
[31] D. Whitman, B.L. Isacks, S.M. Kay, Lithospheric structure and along-strike segmentation of the Central Andean Plateau: seismic Q, magmatism, flexure, topography and tectonics, Tectonophysics 259 (1996) 29–40.
[32] J. Kley, Transition from basement-involved to thin-skinned thrusting in the Cordillera Oriental of southern Bolivia, Tectonics 15 (4) (1996) 763–775.
[33] N. McQuarrie, The kinematic history of the central Andean fold-thrust belt, Bolivia: implications for building a high plateau, GSA Bull. 114 (2002) 950–963.
[34] J.F. Dunn, K.G. Hartshorn, P.W. Hartshorn, Structural styles and hydrocarbon potential of the Sub-Andean thrust belt of southern Bolivia, in: A.J. Tankard, S.R. Suárez, H.J. Welsink (Eds.), Petroleum Basins of South America, American Association of Petroleum Geologists, Tulsa, Oklahoma, 1995, p. 523.
[35] S.H. Lamb, H.M. Bibby, The last 25 Ma of rotational deformation in part of the New Zealand plate-boundary zone, J. Struct. Geol. 11 (4) (1989) 473–492.
[36] S.L. Beck, G. Zandt, S.C. Myers, T.C. Wallace, P.G. Silver, L. Drake, Crustal-thickness variations in the Central Andes, Geology 24 (5) (1996) 407–410.
[37] E. Black, Lithospheric flexure, inheritance and the development of structural styles in the Central Andes, DPhil Thesis, Oxford University (2000).
[38] J.P. Muller, J. Kley, V. Jacobshagen, Structure and Cenozoic kinematics of the Eastern Cordillera, southern Bolivia, Tectonics 21 (5) (2002) (art. 1037).
[39] R.W. Allmendinger, T.R. Zapata, The footwall ramp of the Subandean decollement, northernmost Argentina, from extended correlation of seismic reflection data, Tectonophysics 321 (2000) 37–55.
[40] A. Schneider, Eruptive processes, mineralisation and isotopic evolution of the Los Frailes–KariKari region, Bolivia, PhD Thesis, Imperial College, London (1985).
[41] S. Redwood, R. McIntyre, K–Ar dating of Miocene magmatism and related epithermal mineralization of the northeastern Altiplano of Bolivia, Econ. Geol. 84 (1989) 618–630.

[42] L. Hoke, D. Hilton, S.H. Lamb, K. Hammerschmidt, H. Friedrichsen, ^{3}He evidence for a wide zone of active mantle melting beneath the Central Andes, Earth Planet. Sci. Lett. 128 (1994) 341–355.

[43] M. Springer, Interpretation of the heat-flow density in the Central Andes, Tectonophysics 306 (1999) 377–395.

[44] X. Yuan, S.V. Sobolev, R. Kind, O. Oncken, Andes Seismology Group, New constraints on subduction and collision processes in the Central Andes from comprehensive observations of P to S converted seismic phases, Nature 408 (2000) 958–961.

[45] B. Isacks, Uplift of the Central Andean Plateau and bending of the Bolivian Orocline, J. Geophys. Res. 93 (1988) 3211–3231.

[46] G. Worner, K. Hammerschmidt, F. Henjes-Kunst, J. Lezaun, H. Wilke, Geochronology (^{40}Ar/^{39}Ar, K–Ar and He-exposure ages) of Cenozoic magmatic rocks from Northern Chile (18–22°S): implications for magmatism and tectonic evolution of the Central Andes, Rev. Geol. Chile 27 (2) (2000) 205–240.

[47] D.E. James, I.S. Sacks, Cenozoic formation of the Central Andes: a geophysical perspective, in: B.J. Skinner (Ed.), Geology and Ore Deposits of the Central Andes, vol. 7, Society of Economic Geologists, 1999, pp. 1–25.

[48] J.P. Davidson, S.L. de Silva, Volcanic rocks from the Bolivian Altiplano: insights into crustal structure, contamination, and magma genesis in the Central Andes, Geology 20 (1992) 1127–1130.

[49] S.L. Beck, G. Zandt, The nature of orogenic crust in the central Andes, J. Geophys. Res. 107 (B10) (2002) 2230, doi:10.1029/2000JB000124.